Available online at www.sciencedirect.com
ScienceDirect
Journal of Computational Physics 225 (2007) 2354–2376
JOURNAL OF COMPUTATIONAL PHYSICS
www.elsevier.com/locate/jcp

Estimation of Fekete points

E. Bendito, A. Carmona, A.M. Encinas, J.M. Gesto *

Departament de Matemàtica Aplicada III, Universitat Politècnica de Catalunya, Jordi Girona Salgado, 1-3, 08034 Barcelano, Spain

Received 30 October 2006; received in revised form 19 March 2007; accepted 22 March 2007
Available online 31 March 2007

Abstract

We aim here at presenting a new procedure to numerically estimate the Fekete points of a wide variety of compact sets in $\mathbb{R}^3$. We understand the Fekete point problem in terms of the identification of near equilibrium configurations for a potential energy that depends on the relative position of N particles.

The compact sets for which our procedure works are basically the finite union of piecewise regular surfaces and curves. In order to determine a good initial configuration to start the search of the Fekete points of these objects, we construct a sequence of approximating regular surfaces. Our algorithm is based on the concept of disequilibrium degree, which is defined from a physical interpretation of the behavior of a system of particles when they search for a minimum energy configuration. Moreover, the algorithm is efficient and robust independently of the considered compact set as well as of the kernel used to define the energy. The numerical experimentation carried out suggests that a local minimum can be localized with a computational cost of order less than N^3.

Keywords: Fekete points; Riesz's kernels; Non-linear optimization; Potential energy; Non-smooth surfaces

1. Introduction

The problem of obtaining the Fekete points of a compact set has filled a pre-eminent place in the mathematical research during the last decades. In its original version, the problem consists in determining the position of N points of a compact subset $S \subset \mathbb{R}^2$ that maximize the product of their mutual Euclidean distances. The N-tuples, $\omega_N = \{x_1, \ldots, x_N\}$, that satisfy this property are the so-called *Nth order Fekete points* of S. It is not difficult to verify that these N-tuples minimize in S the functional

$$\mathscr{I}(\omega_N) = \sum_{1 \leqslant i < j \leqslant N} \mathscr{K}(x_i, x_j),$$

where $\mathscr{K}(x_i, x_j) = -\ln|x_i - x_j|$ is the so-called *logarithmic kernel* and $|x_i - x_j|$ is the Euclidean distance between x_i and x_j. The value $\mathscr{I}(\omega_N)$ is the *potential energy* corresponding to the logarithmic kernel when a unitary

* Corresponding author. Tel.: +34 93 401 69 14; fax: +34 93 401 18 25.
E-mail address: jose.manuel.gesto@upc.edu (J.M. Gesto).

0021-9991/$ - see front matter
doi:10.1016/j.jcp.2007.03.017

weight is associated with any point. In the three-dimensional Euclidean space multiple variants of the problem can be formulated by considering different kernels, among which the *Riesz's kernels*, defined as $\mathscr{K}(x_i, x_j) = |x_i - x_j|^{-s}$ with $s > 0$, constitute a family of special interest. In particular, the *Newtonian kernel*, obtained when $s = 1$, has become one of the most relevant cases and its potential energy $\mathscr{I}(\omega_N)$ is named *electrostatic potential energy*. The limit case $s \to 0$ recovers the logarithmic kernel in $\mathbb{R}^3$, whereas the case $s \to \infty$ leads to the so-called *best-packing* problem or *Tammes* problem. On the other hand, the electrostatic phenomenon in $\mathbb{R}^2$ is governed by the logarithmic kernel and the corresponding Fekete points provide "almost ideal" choices of points for polynomial interpolation [20]. Moreover, the usefulness in numerical integration of the Fekete points corresponding to the logarithmic kernel and others on the d-dimensional sphere has been showed by different authors, see for instance [5]. The logarithmic kernel also arises in the study of computational complexity. In particular, the fast generation of near optimal logarithmic energy points for the sphere in $\mathbb{R}^3$ is the focus of one of Smale's "Mathematical problems for the next century" [22]. For a more detailed description of the kernels' properties, see for instance [14].

The determination of the Fekete points of the unit sphere is considered a model of highly non-linear optimization problem with non-linear constraints. In general, only when the constraints are linear or they can be sufficiently well approximated by linear constraints it is reasonable to expect a good behavior of the usual algorithms for optimization problems with constraints. However, even in this case, the convergence ratios result lower than the ones corresponding to free optimization methods. Some authors choose to transform problems like the Fekete point one in optimization problems without constraints by considering a parametrization of the surface [16,18]. In this way, they can use classical optimization techniques such as the *Gradient* method, the *Conjugate Gradient* method, the *Newton* method and the family of *quasi-Newton* methods. Also other techniques like the so-called *Combinatory Optimization* methods have been used, among which stand out the *Simulated Annealing*, the *Tabu Search* and the *Genetic Algorithms* [16]. On the other hand, there exist few results on estimations of the Fekete points of manifolds others than the sphere. In particular, the Fekete points of the torus have been recently studied, see [9,25].

A considerable amount of theoretical and numerical results related to the different versions of the Fekete points problem have been obtained, see for instance [9–13,16,18,19,24], and it has been completely solved in some particular cases. Nevertheless, it is widely assumed that just to obtain a position near to a local optimum for hundreds of points in the sphere requires high computational resources.

In this paper, we propose an algorithm for the numerical estimation of the Fekete points of non-smooth compact sets. Essentially, these compact sets are the finite union of piecewise regular manifolds of different dimensions. We focus in the three-dimensional case, since the estimation of Fekete points is of interest in Chemistry, Biology, Nanotechnology, CAD, etc., see [1,2,9,19]. Moreover, in most of the examples we have considered the Newtonian kernel due to its special relevance, for instance in the electrical and gravitational phenomena, however we also include some examples that consider other kernels. The relation between the electrostatic potential energy of a system of particles and the energy of a distributed charge has been analyzed by several authors. In particular, the results of [12] provide us with a good framework to contrast the quality of the solutions obtained with our algorithm.

We start by describing an algorithm to estimate the Fekete points of smooth surfaces. Next, we analyze the behavior of this algorithm with the prototype problem, the unit sphere. Then, we present a transition case: we estimate the Fekete points of the unit cube by means of the algorithm for smooth surfaces, which requires the use of symmetries to reduce the domain to an open triangle. Finally, we develop a strategy for the estimation of the Fekete points of non-smooth surfaces, and we present several application examples. Throughout the paper the numerical estimation of the Fekete points of a compact set consists in identifying a local minimum from a starting configuration; *i.e.*, in obtaining a sufficiently close configuration to a local minimum in such a way that the Newton's algorithm converges.

2. Smooth surfaces

In this section, we present the fundamentals of our algorithm to estimate the Fekete points of a smooth surface. The basic structure of the algorithm is classical in the sense that each iteration consists in obtaining the advance direction and the step size in a deterministic way.

The ideas behind the algorithm come from Physics. We do not try to answer directly the question about which are the minimum potential energy configurations, but how the points of a non-optimal configuration can advance, in a mechanical sense, to reach a minimum potential energy configuration. The equivalence between minimum potential energy and static stable equilibrium configuration constitutes the key of the method. A mechanical system formed by particles is in equilibrium if the total force that acts on each one of these particles is null. The equilibrium is stable if small perturbations in the position tend to return each particle to its original position, and then this position is a minimum for the potential energy of the system. So, for a given non-optimal configuration, non-equilibrated forces must be acting on the particles and these forces will inevitably induce their movement. We wonder about the character of these forces and of this movement, and about when they will carry the particles to an equilibrium position.

Firstly note that the energy of a system of N unitary particles $x_k \in \mathbb{R}^3$, $k = 1, \ldots, N$, is given by $\mathscr{I} = \frac{1}{2}\sum_{i=1}^{N} V_i$, where $V_i = \sum_{\substack{j=1 \\ j\neq i}}^{N} \mathscr{K}(x_i, x_j)$ is the potential created at x_i by all the other particles. If the particles lie on a regular surface $S \subset \mathbb{R}^3$, then we denote by n_i the normal vector to S at x_i. If we fix the position of $N-1$ particles $\{x_j \in S : j = 1, \ldots, N, j \neq i\}$, then V_i is a function of x_i and the opposite of its gradient, that we denote by $F_i = -\nabla V_i \in T_{x_i}(\mathbb{R}^3)$, represents the repulsive force that acts on the ith particle due to the existence of the rest. We consider $F_i^n = \langle F_i, n_i\rangle n_i$ and $F_i^{\mathrm{T}} = F_i - F_i^n$, the *normal* and *tangent components* to S of the force F_i at x_i, respectively. On the other hand, if $M = S^N$, then $(F_1^{\mathrm{T}}, \ldots, F_N^{\mathrm{T}}) = -\nabla \mathscr{I}_{|M}$ is the steepest descent direction of $\mathscr{I}$ in M, independently of the possible parametrizations of S.

The ith particle is in *equilibrium* on S if $F_i^{\mathrm{T}} = 0$. Therefore, $|F_i^{\mathrm{T}}|$ could be a measure of the disequilibrium degree of that particle on S. Nevertheless, Fig. 1 suggests that an alternative measure of the disequilibrium degree based on the angle between F_i and n_i could result more satisfactory. Effectively, two particles x_i and x_j with $|F_i^{\mathrm{T}}| = |F_j^{\mathrm{T}}|$ can be "more or less equilibrated" on S depending on the angle between the forces F_i and F_j and their corresponding normal vectors n_i and n_j. We define $\frac{|F_i^{\mathrm{T}}|}{|F_i|}$ as the *disequilibrium degree* of the ith particle. The suitability of this choice will be showed clearly throughout the paper.

The following simple proposition establishes that to advance according with this disequilibrium measure descents the energy of the system.

Proposition 2.1. *The direction*

$$w = \left(\frac{F_1^{\mathrm{T}}}{|F_1|}, \cdots, \frac{F_N^{\mathrm{T}}}{|F_N|}\right)$$

is of descent of the energy constrained to M. In addition, every particle contributes to the descent.

Proof. The direction w is obviously compatible with the constraints of the problem, since $w \in T_x(M)$. The result follows from the fact that

$$\langle w, -\nabla \mathscr{I}_{|M}\rangle = \sum_{i=1}^{N} \frac{|F_i^{\mathrm{T}}|^2}{|F_i|} \geqslant 0. \qquad \square$$

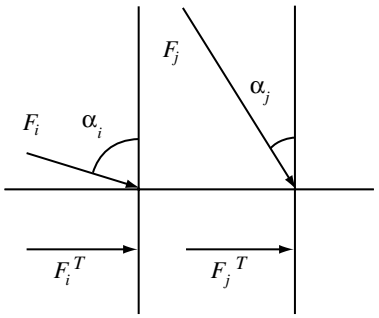

Fig. 1. Disequilibrium degree.

Observe that the direction w does not coincide with the one given by the Gradient method except in very particular cases, for example in the sphere with a great number of particles when they are in stages very close to the equilibrium. On the other hand, as the disequilibrium degree indicator that we propose here is bounded – in fact, it is normalized between 0 and 1 – it allows us to treat each particle only in relation to its own potential equilibrium degree and independently of the relative distance to the rest of particles. The rest of the classical optimization methods, like Conjugate Gradient, Newton or quasi-Newton, choose advance directions that in general do not guarantee that each particle contributes to the descent, which results not very natural in the iterative process.

In any case, the most substantial difference between our approach and the classical methods is that the determination of the advance direction and of the step size is completely independent of the parametrization that has been chosen. Regarding to the direction, that independence has already been made clear. As for the step size some considerations must be made. Given an initial configuration, a unique stationary point for $\mathscr{I}$ must exist such that the particles arrive to it following the direction $w_i = \frac{F_i^{\mathrm{T}}}{|F_i|}$. Consequently, from the point of view of Mechanics, these directions not only can be understood as energy descent directions, but also as the velocity fields of the paths described by the particles in their movement towards the equilibrium. This approach allows us to look at the optimization problem from the dynamic systems perspective. The step size will be chosen by applying an explicit forward Euler method to the ODE system whose solution is precisely these paths. This ODE system is raised in a natural way in the ambient space coordinates and its numerical integration fixes a displacement for each particle in that space. In general, the application of that displacement takes the particles out of the surface S, which generates the need of considering an algorithm to return the particles to the surface in each iteration. Maybe the most versatile and simple method consists in using the gradient field of an implicit representation of the surface. When the surface is described in a parametric form, the composition with the metric allows us to transfer the step magnitude to the parametric space, which solves the return problem.

It is interesting to make some observations about the treatment of the problem from this mechanical point of view. If $x(t) = (x_1(t), \ldots, x_N(t))$ denotes the position of N particles in the instant t, then an equation for the movement of the system on a surface S can be

$$x''(t) = -\nabla\mathscr{I}(x(t)) - cx'(t) + \Phi(x(t), x'(t)).$$

The term $-cx'(t)$, with $c > 0$, represents a dissipative force of viscous nature and $\Phi = (\Phi_1, \ldots, \Phi_N)$ is an additional force that takes into account the interaction between each particle and S. For each $i = 1, \ldots, N$, the normal component of Φ_i, $\Phi_i^n = \rho|x_i'|^2 - F_i^n$, cancels the normal component of F_i and it provides the centripetal force, being ρ the normal curvature in the direction of x_i' at $x_i \in S$. The tangent component Φ_i^{T} considers the friction with S and its expression depends on each particular model. If the friction force is not considered, then it is easy to prove that as $c \to \infty$ the trajectories that solve the above movement equation tend to be the enveloping of the vectors F_i^{T}. Hence, in this case the particles follow the direction of $-\nabla\mathscr{I}_{|M}$. It is possible to propose a friction model such that the corresponding trajectories tend to be the enveloping of the vectors w_i.

Therefore, the search for the minimum of the energy will be carried out by obtaining the paths described by the particles in their movement towards the equilibrium when $c \to \infty$. These ideas belong to the fundamentals of Rational Mechanics and have already been used in the literature by different authors, see for example [17,21,23]. However, in many cases the equilibrium of the particles is purely heuristic and it does not come from the minimization of an explicit functional, and, anyway, the objective is not to localize an equilibrium configuration as a goal in itself, but to arrive to a reasonable level of approximation.

In short, the ODE system that we solve is

$$x' = w.$$

We use the following explicit forward Euler method for its numerical resolution:

$$x^{k+1} = x^k + a\varphi(x^k)w^k,$$

where a is a positive scalar that depends on N, on the kernel and on the surface S, and $\varphi(x^k)$ depends on the current position of all the particles of the system and it allows us to adapt the step size to the difficulty of the different configurations that appear during the calculation. The step size must be reduced when there exist very

close particles in order that they do not "run helter-skelter" breaking the continuity of the movement, whereas if the relative distances grow, the step size can be increased in benefit of the convergence ratio. An appropriate choice is

$$\varphi(x) = \min_{1\leqslant p<q\leqslant N}\{|x_p - x_q|\},$$

according to which $a|w_i|$ represents the fraction of the minimum distance between particles that the ith one advances in each iteration.

The numerical experimentation carried out by the authors confirms that this algorithm converges – in the sense that it localizes an equilibrium position – even for crazy initial positions, for instance the corresponding to confine the N particles in the Nth part of the area of the surface.

3. Unit sphere

The problem of obtaining Fekete points in the unit sphere is probably the most characteristic both for its hardness and for its different applications. This topic was treated from a numerical point of view in the Ph.D. of Zhou [26] and in some works generated around it [18,19]. In [26], minimum energy configurations were obtained for each $N \leqslant 200$ in the case of the Newtonian and logarithmic kernels. Moreover, the author proposed some extrapolation formulae for the minimum energy associated to those kernels, which can also be found in [18]. The algorithms used in these works are quasi-Newton after the elimination of the constraints by means of the stereographic projection. More recently new results have been obtained by Womersley [24] by using similar techniques.

In this section, we present the application of our algorithm in the unit sphere, we analyze its properties and we evaluate the quality of the obtained solutions. After the generation of an arbitrary initial configuration x^0 of N different points on the sphere, the steps of the kth iteration of our algorithm are

- Calculate the advance direction w^{k-1}.
- Calculate $\hat{x}^k = x^{k-1} + ad_{k-1}w^{k-1}$.
- Obtain the kth configuration: $x_i^k = \frac{\hat{x}_i^k}{|\hat{x}_i^k|}$.

Here, d_{k-1} represents the minimum distance between two points of the (k-1)th configuration, that is obtained as a byproduct of the advance direction calculation. For the kernels we are interested in, the most expensive step of the iterative process is precisely the calculation of this direction, that involves order N^2 operations. In Table 1 we show reference values for the coefficient a for some kernels in the sphere.

To study the convergence of our algorithm, we use as a measure of the error the maximum disequilibrium degree of the particles; *i.e.*, $\max_{1\leqslant i\leqslant N}|w_i|$. If we analyze the evolution of the error with respect to the iteration number, we observe that a linear convergence ratio is systematically attained after a first highly non-linear stage. When the linear stage is reached the particles can be supposed to be sufficiently close to a stationary point, in the sense that from this moment the Newton's algorithm can be used with guaranty of convergence. In the sequel, we will use indistinctly the terms "near local-minimum configuration" and "configuration in linear tendency" to describe this stage of the calculation.

Fig. 2a illustrates the behavior of the error for a configuration of 1000 particles with the Newtonian kernel. Fig. 2b displays the evolution of the difference between the energy corresponding to the extrapolation formula given in [18] and the energy computed with our algorithm. We must note that the energy given by the formula, in spite of being accurate, can be improved very quickly. In fact, this happens long before the linear tendency is reached.

Table 1
Reference values for the coefficient a

Kernel	Logarithmic	Newtonian	Riesz $s = 2$	Riesz $s = 3$
a	8	1	0.1	0.02

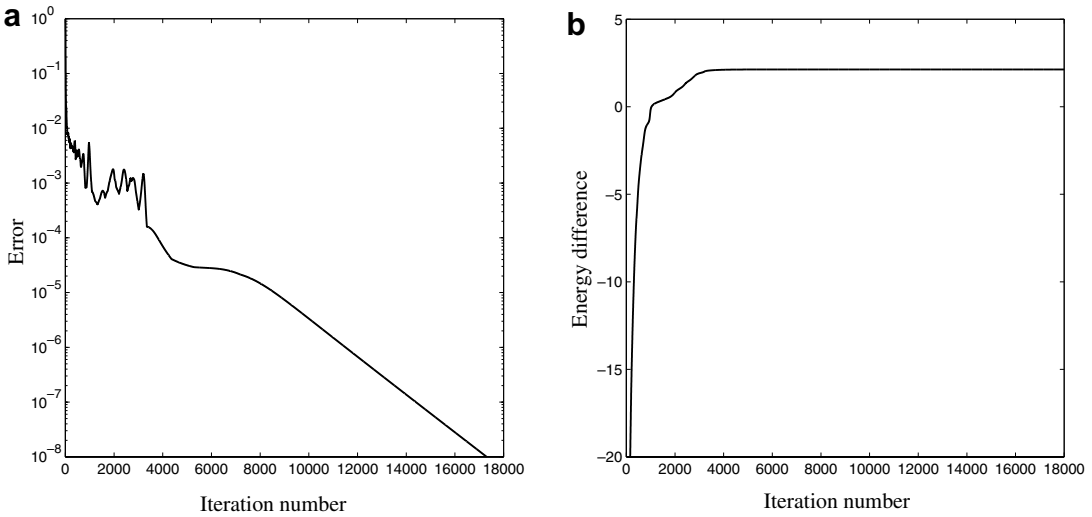

Fig. 2. The behavior of the algorithm.

Fig. 3 shows the initial and final configurations of the non-linear stage for the previous case as well as the Dirichlet cells of both configurations. The initial configuration was generated randomly by adjusting the distribution of the particles to a uniform probability density on the sphere. We must note that the energy produced by the initial configuration is 500144.450659 and after the iterative process the energy value is 482534.789049, which represents only a 3.5% of decrease. On the other hand, the algorithm shows a high efficiency, since the time required to reach the linear tendency was around 15 min and to surpass the extrapolated energy value required only around 2 min with a conventional Pentium IV processor of 2.54 GHz and 512 Mb of RAM.

Fig. 4 shows a configuration of, 5000 particles when the linear tendency has been attained, which required approximately 20 h. With a configuration of 50000 particles, and without considering symmetries, the time required to improve the energy corresponding to the extrapolation formula was of approximately 15 h.

Next we validate our algorithm by comparing the results provided by it with the ones available in the literature. With this aim, we have performed a test that consists in localizing the best minimum obtained from 1000 different random initial positions. Womersley developed a similar test for the Newtonian kernel with $N = (m+1)^2$ and m up to 80, see [24]. In Table 2, we show the number of starting positions that lead to

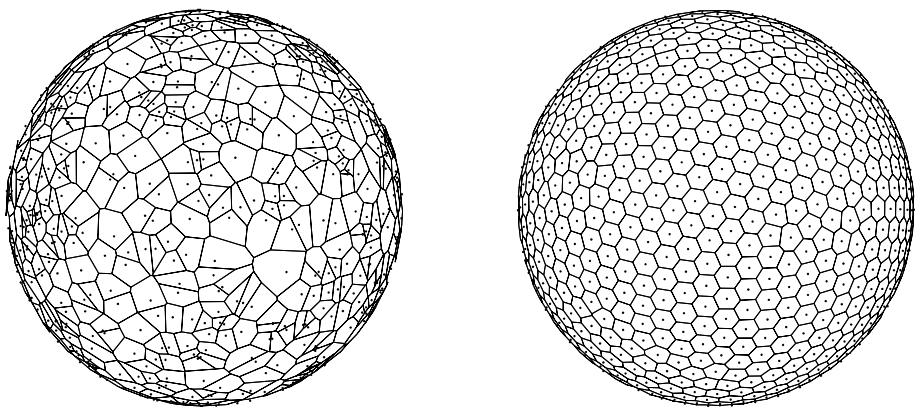

Fig. 3. One thousand particles and its Dirichlet cells for the iterations 0 and 8000.

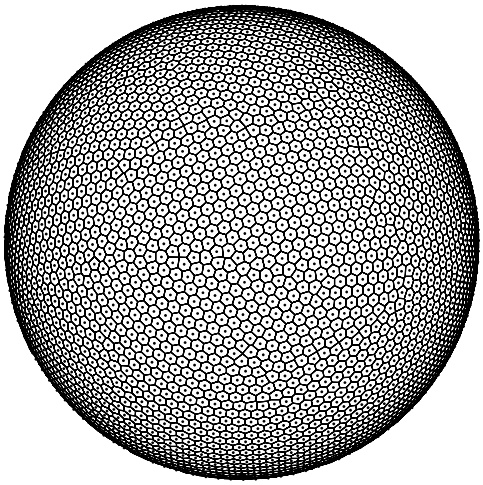

Fig. 4. A beautiful configuration and the Dirichlet cells for $N = 5000$.

the best energy value, n_g, the number of different local minima identified in 1000 runs, n_l, and the corresponding best electrostatic potential energy, $\mathscr{I}$. We have stopped the test when in 1000 runs no one of the local minima obtained gives the energy value calculated by Womersley, which happens for $N = 256$. For this number of particles we have found 995 different local minima with a best energy value of 30506.79464064, whereas Womersley obtains a configuration with a value of 30506.68751585.

Fig. 5 (left), extracted from [24], displays the distribution of local minima obtained by Womersley for $N = 169$ and 100000 runs, whereas Fig. 5 (right) shows the distribution obtained by us in the same case with 1000 runs.

Although the results obtained with our algorithm suggest an average cost of order less than N^3 to attain a configuration in linear tendency, it is still necessary more numerical experimentation to confirm it. It must be considered that in such a non-linear problem, some fluctuations in the cost are natural. For instance, for fixed N similar initial configurations could require different calculation times, whereas configurations with more particles than others could require less iterations. It is clear that the memory requirements are of order N. Moreover, the tests carried out until now confirm the robustness of the algorithm.

To obtain good equilibrium configurations for a great number of particles without an increase of the computational resources we can use the symmetries of the sphere. The geodesic lattices are good initial configurations that take into account that symmetries. In particular, we consider families of truncated icosahedron, which corresponds to use 120 symmetries. Although the geodesics constitute an excellent family

Table 2
Validation of the algorithm

N	n_g	n_l	$\mathscr{I}$
4	1000	1	$3.674234614175 \times 10^0$
9	1000	1	$2.575998653127 \times 10^1$
16	770	2	$9.291165530254 \times 10^1$
25	1000	1	$2.438127602988 \times 10^2$
36	1000	1	$5.291224083754 \times 10^2$
49	1000	1	$1.011557182654 \times 10^3$
64	846	6	$1.765802577927 \times 10^3$
81	461	8	$2.878522829664 \times 10^3$
100	439	27	$4.448350634331 \times 10^3$
121	55	82	$6.586121949584 \times 10^3$
144	188	158	$9.414371794460 \times 10^3$
169	37	498	$1.306800645113 \times 10^4$
196	2	837	$1.769346054808 \times 10^4$
225	13	904	$2.344943646067 \times 10^4$

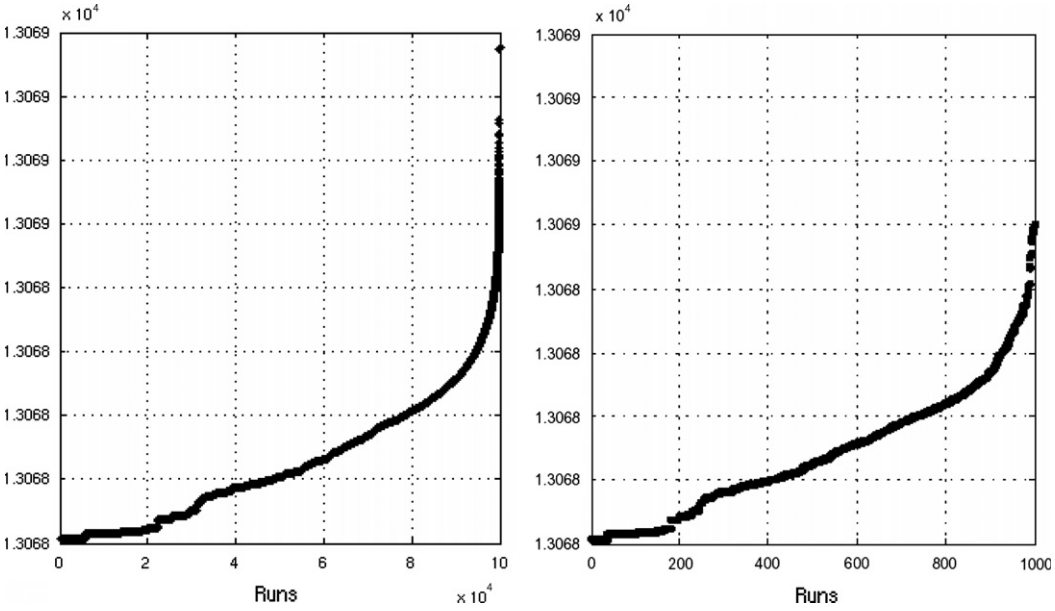

Fig. 5. Distribution of local minima for $N = 169$. The left graph was extracted from [24].

of initial configurations, they do not present a uniform density of points. This is due to the projection that takes the points from the faces of the icosahedron to the sphere. In this conditions, our algorithm basically smooths the density, as can be seen in Fig. 6. In this figure we represent the initial and final positions of the points corresponding to a face of the original icosahedron for a configuration with 12002 particles in total.

In Fig. 7, we present the convergence curves for several configurations whose initial positions are defined by different frequency geodesic lattices. The total number of particles for each one of the seven cases considered are (1) $N = 4322$, (2) $N = 12002$, (3) $N = 27002$, (4) $N = 52922$, (5) $N = 100922$, (6) $N = 201722$, (7) $N = 300002$. Note that the evolution of the error is very smooth even before the final linear tendency is attained. A reason for that is the great quality of the initial configurations. Moreover, it must be observed that all the geodesics of this family start with approximately the same error. This fact can be used to perform an analysis of the cost in similar conditions. If we consider the reference error $\mathrm{e} = 5 \times 10^{-3}$, we can obtain in each case the number of necessary iterations to attain e. This is shown in Fig. 7 as well as a simple interpolation of the data.

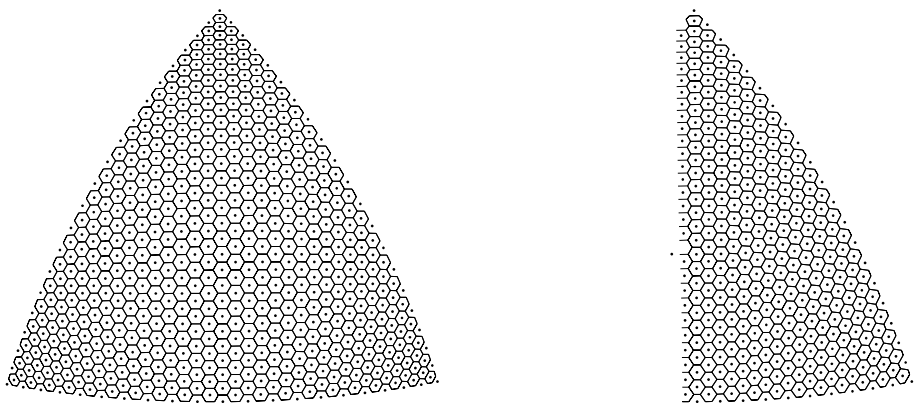

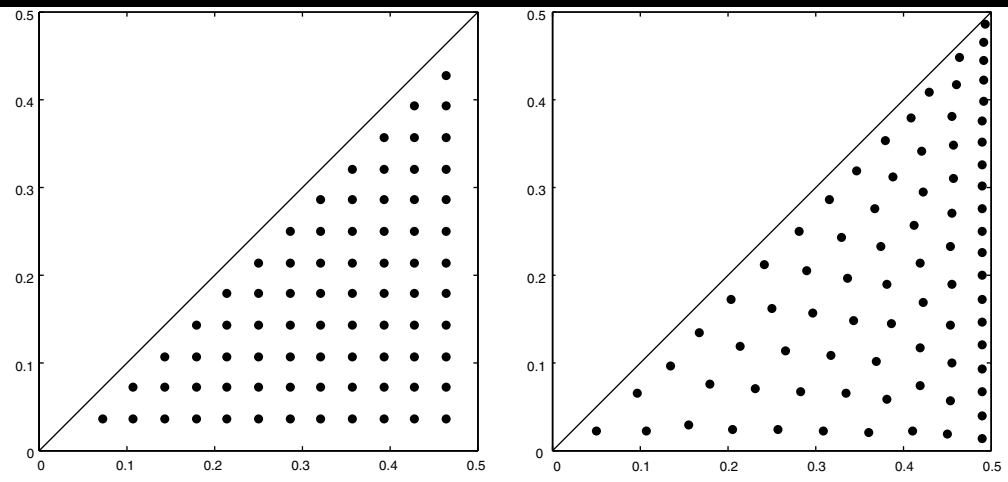

Fig. 8. Initial and final configuration for 78 particles in the triangle.

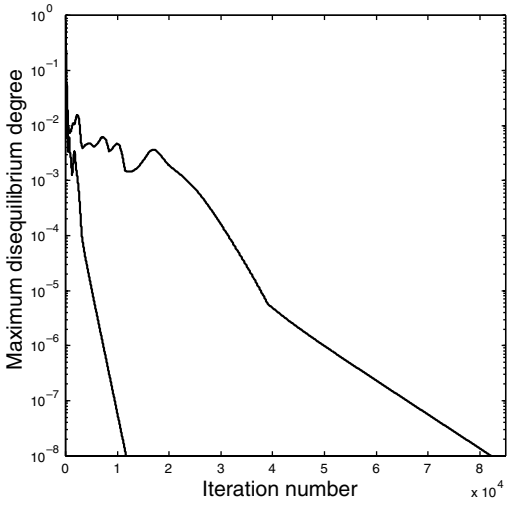

Fig. 9. Comparison between the gradient direction and the w direction.

is shown in Fig. 9. In each case, the step size was determined according to the mechanical criterion described in Section 2 and it was chosen as fast as possible keeping the convergence. We want to observe that the calculations performed with the gradient direction do not correspond to the standard Gradient method, in which the step size is typically obtained by means of the so-called *line search* procedure.

The fact that both directions lead to the same configuration from a given initial position is casual. In most cases, the final local minima are different, but the direction w arrives sooner to the linear tendency and the final linear convergence ratio is higher, with rare exceptions. To complete this study we have computed the average ratio between the number of necessary iterations to attain a maximum disequilibrium degree of 10^{-5} following the gradient direction, which is denoted by $n_{\vec{w}}$, and following the direction w, which is denoted by n_w, for different number of points in the triangle, N_t. The results are displayed in Table 3. The average ratio has been obtained from 100 runs for each N_t, starting from the same random initial positions for both directions, and, as above, taking a step size as fast as possible keeping the convergence. Among the 1000 total runs, only in five of them the gradient direction was faster than the direction w. Moreover, the average ratio corresponding to these five cases is only 0.8. Although N_t varies in a short range, the results suffice to see that the ratio tends to increase with N_t, which in general happens in any compact set. Uniquely the geometry of the sphere makes both directions "equivalent", in the sense that to attain the linear tendency requires approximately the same average number of iterations.

Fig. 10 shows a near local-minimum distribution in a face of the unit cube obtained by our algorithm for a total quantity of 47520 particles, which corresponds to $N_t = 990$. The linear tendency is reached in 40000 iterations.

Clearly, the equilibrium configuration showed in Fig. 10 cannot be considered a good estimation of the Fekete points of a cube. The use of symmetries implies certain constraints. In our starting position, we have placed all the particles in the interior of the open triangle, and hence in the final configuration there are no points on the edges of the cube. If we want charges on the edges in the final configuration, we need to decide how many charges we have to place on the boundary of the triangle in the starting position. So, it seems necessary to complete the above algorithm to tackle the problem of the numerical estimation of the Fekete points of non-regular objects.

Table 3
Average behavior of the gradient versus the w direction

N_t	5	10	15	20	25	30	35	40	45	50
$\frac{n_{\vec{w}}}{n_w}$	2.3	4.1	4.3	5.4	6.2	6.2	7.5	9.3	8.8	9.1

5.1. W-compact sets

We would like to emphasize the generality of the sets where we can obtain good configurations for the Fekete point problem. The most relevant characteristic of the family of sets that we consider is, roughly speaking, the piecewise smoothness in a wide sense. In particular, we admit the finite union of surfaces with curves.

Let $\mathscr{S} \subset \mathbb{R}^3$ be a connected compact set with two-dimensional Lebesgue measure. Let us also consider the subsets:

$$A = \{x \in \mathscr{S} : \mathscr{S} \text{ is a differentiable 2-manifold at } x\},$$

and

$$B = \{x \in \mathscr{S} \setminus A : \mathscr{S} \setminus A \text{ is a differentiable 1-manifold at } x\}.$$

We call *face*, *edge* and *vertex* of $\mathscr{S}$ each connected component of A, B and $\mathscr{S} \setminus (A \cup B)$, respectively. We say that $\mathscr{S}$ is a *W-compact set*, when it has a finite number of faces, edges and vertices and in addition $\mathscr{S} \setminus A$ is a set with 1-dimensional Lebesgue measure and $\mathscr{S} \setminus (A \cup B)$ has null Lebesgue measure.

We work with W-compact sets such that for each $n \geqslant m_0$ the number of connected components of $D_n = \{x \in \mathbb{R}^3 : d(x, \mathscr{S}) = \frac{1}{n}\}$ remains constant and equals the number of connected components of $\mathbb{R}^3 \setminus \mathscr{S}$, where d represents the Euclidean distance in $\mathbb{R}^3$. Then, there exists a sequence of connected compact differentiable surfaces without boundary, $\{S_n\}_{n=1}^{\infty}$, that tends to $\mathscr{S}$, in the sense that for each $x \in \mathscr{S}$, $d(x, S_n) \to 0$ and also the sequence $\{\max_{x \in S_n}\{d(x, \mathscr{S})\}\}_{n=1}^{\infty} \to 0$.

Observe that the surfaces S_n can be built from D_n by connecting all its connected components and smoothing the final surface. Specifically, we connect two components as follows. Let us consider a regular point x on a face that belongs to the boundary of two connected components of $\mathbb{R}^3 \setminus \mathscr{S}$. Then we can choose r_n such that $D_n^1 = \{x \in \mathbb{R}^3 : d(x, \mathscr{S}_n^1) = \frac{1}{n}\}$ has one connected component less than D_n, where $\mathscr{S}_n^1 = \mathscr{S} \setminus \{B(x, r_n) \cap \mathscr{S}\}$.

Now, we can analyze the construction of good initial positions for the Fekete point problem for W-compact sets. It is well known that if a compact set $K \subset \mathbb{R}^3$ is the intersection of a decreasing sequence of compact sets $\{K_n\}_{n=1}^{\infty}$, then the measures that minimize the Newtonian energy of K_n weakly* converge to the measure that minimizes the Newtonian energy of K. Taking into account that the Newtonian optimal measure of K_n has its support on the outer boundary $\partial_0 K_n$, then the electrostatic optimal measures of the boundaries $\partial_0 K_n$ weakly* converge to the electrostatic optimal measure of $\partial_0 K$. On the other hand, the discrete measure supported by the Fekete points of $\partial_0 K_n$ weakly* converges to the optimal measure of $\partial_0 K_n$.

These results suggest that a sufficiently well equilibrated configuration of N points on a sufficiently good approximating surface can be used to construct a good initial position to start the search of the Nth order Fekete points of $\mathscr{S}$. Our intention here is to show evidence of the effectiveness of this numerical approach even in contexts that are not necessarily under the hypotheses of the classical theorems. For other results about approximation of solutions of the energy minimization problem considering several kernels, measures sets and support spaces see [3,8,14].

5.2. Regular approximation to W-compact sets

From a practical point of view, we need an effective technique to construct a sequence of approximating surfaces $\{S_n\}_{n=1}^{\infty}$ of a given W-compact set. Among the different procedures that could be used, we want to mention one based on a technique of composition of implicit functions widely used in different areas, especially in Computer Graphics, see for instance [4]. This method provides global implicit equations to describe very general geometries.

We present here a systematic analysis of three fundamental cases associated to the approximation of boundaries of open sets, surfaces with boundary and curves. Then, the feasibility of the approximation of a wide variety of W-compact sets that are the combination of these three cases by means of more general composition operations can be easily proved.

5.2.1. Case 1: boundaries of open sets

Next, we analyze the approximation process to the boundaries of open sets that can be described in the form

$$\Omega = \left\{ x \in \mathbb{R}^3 : \max_{1 \leqslant i \leqslant k} \{G_i(x)\} < 1 \right\},$$

where $G_i : \mathbb{R}^3 \to \mathbb{R}^+$, $i = 1, \ldots, k$, $k \in \mathbb{N}$ are sufficiently smooth functions. Let we consider the sequence $\{A_n\}_{n=1}^{\infty}$ of open sets defined for each $n \in \mathbb{N}$ by

$$A_n = \left\{ x \in \mathbb{R}^3 : \sum_{i=1}^{k} G_i(x)^n < 1 \right\}.$$

Lemma 5.1. *The sequence $\{A_n\}_{n=1}^{\infty}$ increases to Ω, that is, $A_n \uparrow \Omega$. Moreover, the sequence $\{\partial A_n\}_{n=1}^{\infty}$ tends to $\partial\Omega = \{x \in \mathbb{R}^3 : \max_{1 \leqslant i \leqslant k} \{G_i(x)\} = 1\}$.*

Proof. Let us consider $x \in A_n$. Then for each $i \in \{1, \ldots, k\}$, $0 \leqslant G_i(x) < 1$, and hence $\sum_{i=1}^{k} G_i(x)^{n+1} < \sum_{i=1}^{k} G_i(x)^n < 1$ and $x \in A_{n+1}$. On the other hand, if $x \in \Omega$ and $\Phi_x = \max_{1 \leqslant i \leqslant k} \{G_i(x)\}$, then $0 \leqslant \Phi_x < 1$ and $\sum_{i=1}^{k} G_i(x)^{\ell} \leqslant k\Phi_x^{\ell}$, $\ell \in \mathbb{N}$. Therefore, if $n_x = \min\{j \in \mathbb{N} : k\Phi_x^j < 1\}$ then for each $n \in \mathbb{N}$ such that $n \geqslant n_x$, $x \in A_n$. □

The following simple example illustrates this case. The sequence of sets

$$\partial A_n = \{(x, y, z) \in \mathbb{R}^3 : x^{2n} + y^{2n} + z^{2n} = 1\},$$

goes from the sphere to the cube

$$\partial\Omega = \{(x, y, z) \in \mathbb{R}^3 : \max\{x^2, y^2, z^2\} = 1\},$$

when n goes from 1 to ∞.

5.2.2. Case 2: surfaces with boundary

We consider now the approximation to connected compact surfaces with boundary that can be described in the form

$$\Gamma = \left\{ x \in \mathbb{R}^3 : G(x) = 0, H(x) \leqslant 0 \right\},$$

where $G, H : \mathbb{R}^3 \to \mathbb{R}$ are sufficiently smooth functions. Consider also the sequence $\{A_n\}_{n=1}^{\infty}$ of open sets defined for each $n \in \mathbb{N}$ by

$$A_n = \{x \in \mathbb{R}^3 : nG(x)^2 + H(x) > 0\}.$$

Lemma 5.2. *The sequence $\{A_n\}_{n=1}^{\infty}$ increases to $\mathbb{R}^3 \setminus \Gamma$. Moreover, the sequence $\{\partial A_n\}_{n=1}^{\infty}$ tends to Γ.*

Proof. If $x \in A_n$, then $(n+1)G(x)^2 + H(x) \geqslant nG(x)^2 + H(x) > 0$ and hence $x \in A_{n+1}$. On the other hand, if $x \in \mathbb{R}^3 \setminus \Gamma$ then either $G(x)^2 > 0$ or $H(x) > 0$. In any case, if $n_x = \min\{j \in \mathbb{N} : jG(x)^2 > -H(x)\}$ then for each $n \in \mathbb{N}$ such that $n \geqslant n_x$, $x \in A_n$. □

Observe that $\partial\Gamma \subset \partial A_n$ for each $n \in \mathbb{N}$. In addition, if Γ is a surface without boundary of the form $\Gamma = \{x \in \mathbb{R}^3 : G(x) = 0\}$, the above result is also true taking $H = -1$.

As an example of this situation, we can mention the approximation of the unit disc

$$\Gamma = \{(x, y, z) \in \mathbb{R}^3 : z = 0, x^2 + y^2 - 1 \leqslant 0\},$$

by means of the sequence of oblate ellipsoids

$$\partial A_n = \{(x, y, z) \in \mathbb{R}^3 : nz^2 + x^2 + y^2 - 1 = 0\}.$$

5.2.3. Case 3: curves with boundary

We focus here in the approximation to connected compact curves with boundary that can be described in the form

$$C = \{x \in \mathbb{R}^3 : G(x) = 0, H(x) = 0, J_1(x) \leqslant 0, J_2(x) \leqslant 0\},$$

where $G, H, J_1, J_2 : \mathbb{R}^3 \to \mathbb{R}$ are sufficiently smooth functions verifying that the set $\{x \in \mathbb{R}^3 : J_1(x) > 0, J_2(x) > 0\}$ is empty. Consider also the sequence $\{A_n\}_{n=1}^{\infty}$, of open sets defined for each $n \in \mathbb{N}$ by

$$A_n = \{x \in \mathbb{R}^3 : nG(x)^2 + nH(x)^2 - J_1(x)J_2(x) > 0\}.$$

Lemma 5.3. *The sequence $\{A_n\}_{n=1}^{\infty}$ increases to $\mathbb{R}^3 \setminus C$. Moreover, the sequence $\{\partial A_n\}_{n=1}^{\infty}$ tends to C.*

Proof. If $x \in A_n$, then

$$(n+1)G(x)^2 + (n+1)H(x)^2 - J_1(x)J_2(x) > nG(x)^2 + nH(x)^2 - J_1(x)J_2(x) > 0$$

and hence $x \in A_{n+1}$. On the other hand, if $x \in \mathbb{R}^3 \setminus C$ then either $G(x)^2 + H(x)^2 > 0$ or $J_1(x)J_2(x) < 0$. In any case, if $n_x = \min\{j \in \mathbb{N} : j(G(x)^2 + H(x)^2) > J_1(x)J_2(x)\}$ then $x \in A_n$, for each $n \in \mathbb{N}$ such that $n \geqslant n_x$. □

Observe that $\partial C \subset \partial A_n$ for each $n \in \mathbb{N}$. Moreover, if $\partial C = \emptyset$ it suffices to take $J_1 = J_2 = -1$, whereas if $\partial C \subset \{J_1 = 0\}$, it suffices to take $J_2 = -1$.

The approximation of the segment

$$C = \{(x, y, z) \in \mathbb{R}^3 : y = 0, z = 0, x - 1 \leqslant 0, -x - 1 \leqslant 0\},$$

by means of the sequence of prolate ellipsoids

$$\partial A_n = \{(x, y, z) \in \mathbb{R}^3 : ny^2 + nz^2 + x^2 - 1 = 0\}$$

illustrates this case.

5.3. The energy restricted to a W-compact set

Let $\mathcal{S}$ be a W-compact set. For each $x \in \mathcal{S}$, we can consider the set $\mathscr{C}_x$ of all the differentiable curves contained in $\mathcal{S}$ with origin in x. Under this conditions, we define the *mobility set* of x on $\mathcal{S}$, $\mathscr{T}_x(\mathcal{S})$, by

$$\mathscr{T}_x(\mathcal{S}) = \{\mathsf{t} \in \mathbb{R}^3 : t \text{ is the unitary tangent vector at } x \text{ of } \gamma \in \mathscr{C}_x\}.$$

If x is on a face of $\mathcal{S}$, then its mobility set generates the tangent plane to $\mathcal{S}$ at x, $T_x(\mathcal{S})$.

If $f : \mathbb{R}^3 \to \mathbb{R}$ is a regular function in $x \in \mathcal{S}$, let us consider the scalar

$$p = \max_{\mathsf{t} \in \mathscr{T}_x(\mathcal{S})} \{-\langle \nabla f(x), \mathsf{t} \rangle\},$$

and the set $\mathsf{t}_x(\mathcal{S})$ defined by

$$\mathsf{t}_x(\mathcal{S}) = \begin{cases} \{\mathsf{t} \in \mathscr{T}_x(\mathcal{S}) : -\langle \nabla f(x), \mathsf{t} \rangle = p\}, & \text{if } p > 0, \\ \{\mathsf{0}\}, & \text{if } p \leqslant 0. \end{cases}$$

Under these conditions, we define the set

$$\mathscr{G}_x(f, \mathcal{S}) = p\mathsf{t}_x(\mathcal{S}),$$

as the *steepest descent set* of $f_{|\mathcal{S}}$ at x.

Let us note that even when $\mathcal{S}$ is a W-compact set, $\mathscr{G}_x(f, \mathcal{S})$ can contain a non-numerable quantity of elements. For example, if x is the vertex of a revolution half cone and $-\nabla f(x)$ points towards the interior of the cone in the direction of its axis, then $\mathsf{t}_x(\mathcal{S})$ is $\mathscr{T}_x(\mathcal{S})$.

If $x \in \mathscr{S}$, then we define the set

$$\mathscr{N}_x(\mathscr{S}) = \{\mathsf{q} \in S^2 : \langle \mathsf{q}, \mathsf{t}\rangle \leqslant 0 \text{ for each } \mathsf{t} \in \mathscr{T}_x(\mathscr{S})\},$$

as the *normal set* to $\mathscr{S}$ at x. Observe that if $\nabla f(x) \neq 0$ and $-\frac{\nabla f(x)}{|\nabla f(x)|} \in \mathscr{N}_x(\mathscr{S})$ then x is in equilibrium on $\mathscr{S}$ and hence we say that x is a *generalized stationary point* of $f_{|\mathscr{S}}$. Let us note that if $\mathscr{T}_x(\mathscr{S})$ has only one element then $\mathscr{N}_x(\mathscr{S})$ is a closed hemisphere. Hence, in general, $\mathscr{N}_x(\mathscr{S})$ is the intersection of all the closed hemispheres associated with each $\mathsf{t} \in \mathscr{T}_x(\mathscr{S})$. If x belongs to a face, then $\mathscr{N}_x(\mathscr{S})$ has only two opposite points that define the normal direction to the face. In the simple case in which $\mathscr{S}$ is the boundary of a convex polyhedron, if x belongs to an edge, then $\mathscr{N}_x(\mathscr{S})$ is an arc of circumference, and if x is a vertex where r faces meet, then $\mathscr{N}_x(\mathscr{S})$ is the convex spherical r-gon whose vertices are the outer normal vectors to these faces. In a general case $\mathscr{N}_x(\mathscr{S})$ can admit multiple forms. If $\mathscr{N}_x(\mathscr{S})$ has non-null bi-dimensional measure, then x is necessarily a vertex, but no more general results exist. For example, $\mathscr{N}_x(\mathscr{S})$ can be the empty set in a vertex. A point $x \in \mathscr{S}$ such that $\mathscr{N}_x(\mathscr{S}) = \emptyset$ have more freedom of movement than the points on a face, because x is a generalized stationary point of $f_{|\mathscr{S}}$ only when x is a stationary point of f.

For a given $x \in \mathscr{S}$, the computation of $\mathscr{G}_x(f, \mathscr{S})$ requires in general to solve an optimization problem. However, its resolution can be reduced to a finite number of trivial verifications except when x belongs to the boundary of a face C such that $\overline{C}$ is not regular at x, in which case *ad hoc* techniques must be used. If $x \in \mathscr{S}$ belongs to a face, then the unique element in $\mathscr{G}_x(f, \mathscr{S})$ is $-Pr_{T_x(\mathscr{S})}\nabla f(x)$; *i.e*, the projection of $-\nabla f(x)$ on the tangent plane $T_x(\mathscr{S})$. Otherwise, let us suppose, for instance, that x is a vertex belonging to the boundaries of the faces $h_1, \ldots, h_r$ and to the boundaries of the edges $e_1, \ldots, e_s$, and that $\overline{h_j}$ are regular at x. We denote by π_j the tangent plane to $\overline{h_j}$ at x and by t_i the unitary tangent vector to the edge e_i at x. Consider now the closed half straight lines l_i generated by t_i and the closed subsets $\hat{\pi}_j \subset \pi_j$ that are delimited by the two half straight lines $l_{j_1}, l_{j_2} \subset \pi_j$. Then it suffices to find the best approximation of $x - \nabla f(x)$ to the r sets $\hat{\pi}$ and to the m half straight lines l that do not belong to any $\hat{\pi}$. For this we calculate $y^j = -Pr_{\pi_j}\nabla f(x)$, and we generate a list L containing all the scalars $|y^j|$ such that $x - y^j \in \hat{\pi}_j$ and the scalars $-\langle \nabla f(x), \mathsf{t}\rangle$ corresponding to the m half straight lines referred above. In this conditions, p is the maximum element in L, and $\mathsf{t}_x(\mathscr{S})$ is directly obtained. Other simpler cases can be analogously solved.

With regards to the Fekete point problem, we can choose any element in $\mathscr{G}_x(V_i, \mathscr{S})$ as F_i^{T}. On the other hand, the different definitions made above can be directly generalized. If $\mathscr{M} = \mathscr{S}^N$ and $x = \{x_1, \ldots, x_N\} \in \mathscr{M}$, then we denote the mobility set of the configuration $x \in \mathscr{M}$ by $\mathscr{T}_x(\mathscr{M}) = \mathscr{T}_{x_1}(\mathscr{S}) \times \ldots \times \mathscr{T}_{x_N}(\mathscr{S})$. The sets $\mathsf{t}_x(\mathscr{M})$, $\mathscr{G}_x(\mathscr{I}, \mathscr{M})$ and $\mathscr{N}_x(\mathscr{M})$ can be analogously defined.

5.4. The algorithm

With the background of the previous subsections, we can describe the main steps of our algorithm for the estimation of the Fekete points of W-compact sets. We want to point out that an important part of that background has the objective of producing good initial positions to obtain good local energy minima on a non-smooth object.

Our approach has two different parts. The first one has a purely geometric character, and it comprises the description of the W-compact set $\mathscr{S}$, the construction of its approximating regular surfaces and the choice of a procedure to project points from one of these objects to another. The second part consists in an iterative algorithm for the search of Fekete points, and it includes the determination of an advance direction, a step size and a geometric criterion to return the points to the object.

We have presented above a useful technique to define approximating implicit surfaces. Independently of the procedure used for the generation of these surfaces, we must note that to obtain good initial positions it is necessary to design an *ad hoc* approximation strategy for each considered problem, in the sense that the number of intermediate approximating surfaces and their degree of approximation to $\mathscr{S}$ must be adapted to the specific geometric difficulties of $\mathscr{S}$ and to the number of points. In the following section, we present a variety of examples that show how this strategy can be developed in a simple way in many practical cases.

On the other hand, the closest point technique provides a very general way of projecting points from a set to another. However, this technique can project two different points to the same position and it requires to solve a non-trivial optimization problem. In many cases to project along the normal direction can also be an inter-

esting method. Although this can be done efficiently by means of the one-dimensional Newton's method, it is possible that this direction does not intersect with the involved set. In any case, from our experience, any reasonable projection procedure produces in practice good results. Let us also note that any projection method has always a computational cost of order N -in each iteration-, and hence it is a minor problem. All these comments are also applicable to the return algorithm corresponding to the iterative process.

Although the descent algorithm in an approximating surface is in linear tendency, the potential energy will be far from any local minimum after the projection to the next surface. Therefore, when we are on an approximating surface, we only search configurations in a reasonably good equilibrium state. It can be enough to take a maximum disequilibrium degree between 10^{-2} and 10^{-3}. In these conditions, the computational cost of the process of obtaining a good initial position on $\mathscr{S}$ is not relevant in comparison with the computational cost of searching a near local-minimum configuration on $\mathscr{S}$. To apply the descent algorithm in $\mathscr{S}$, F_i^{T} must be calculated as indicated in the previous subsection. However, some specific considerations must be made. If a particle moving on a face of $\mathscr{S}$ crosses its boundary, it must be projected to this boundary before F_i^{T} is updated. In the new position, F_i^{T} will decide whether the particle will move along the boundary, will return to the original face or will go to other face. An analogous procedure must be carried out if a particle moving along an edge of $\mathscr{S}$ crosses its boundary.

We finish this section by presenting a scheme of our proposal to numerically estimate the Fekete points of a W-compact set $\mathscr{S}$:

1. Generate a good initial configuration on $\mathscr{S}$.
   1.1. Define r approximating regular surfaces S_k, $1 \leqslant k \leqslant r$.
   1.2. Generate a random configuration of N points on S_1.
   1.3. For each k, $1 \leqslant k \leqslant r$, obtain a configuration in a reasonably good equilibrium state on S_k by means of the descent algorithm and project it to the next surface. The last projection is from S_r to $\mathscr{S}$.
2. Starting from the last configuration, apply the descent algorithm to obtain a configuration in linear tendency on $\mathscr{S}$ taking into account its non-smoothness.

We want to remark that the total computational cost of the process of obtaining a near local-minimum configuration on a W-compact set $\mathscr{S}$ is essentially the same in all the cases that we have considered, and this cost seems to be less that N^3.

6. Some examples

The following examples show the versatility of our algorithm. We have included some examples with academic interest and others of playful character but with evident difficulties with regards to the obtaining of equilibrium configurations.

6.1. Unit cube

For this case, we use approximating regular surfaces implicitly described by

$$f_p(x,y,z) = \mathrm{e}^{p(x^2-0.25)} + \mathrm{e}^{p(y^2-0.25)} + \mathrm{e}^{p(z^2-0.25)} = 1,$$

with $p \in \mathbb{R}^+$. More explicitly, we work with two approximating surfaces defined by p=15,30, respectively.

Fig. 11 illustrates the general behavior of our algorithm for non-smooth surfaces. In the upper part we show the final configurations – with a maximum disequilibrium degree of 10^{-2} – corresponding to the approximating regular surfaces with $N = 10537$. As we can see, the approximating surface with $p = 30$ has a noticeable accumulation of particles in the most curved zones, which correspond to the edges and vertices of the final cube. The projection between surfaces has been carried out along the direction of the normal vector by means of the Newton's algorithm. In the same figure (down), a near local-minimum configuration on the unit cube $\mathscr{S}$ and the corresponding convergence graph are displayed. Let us note that we have not used symmetries in this

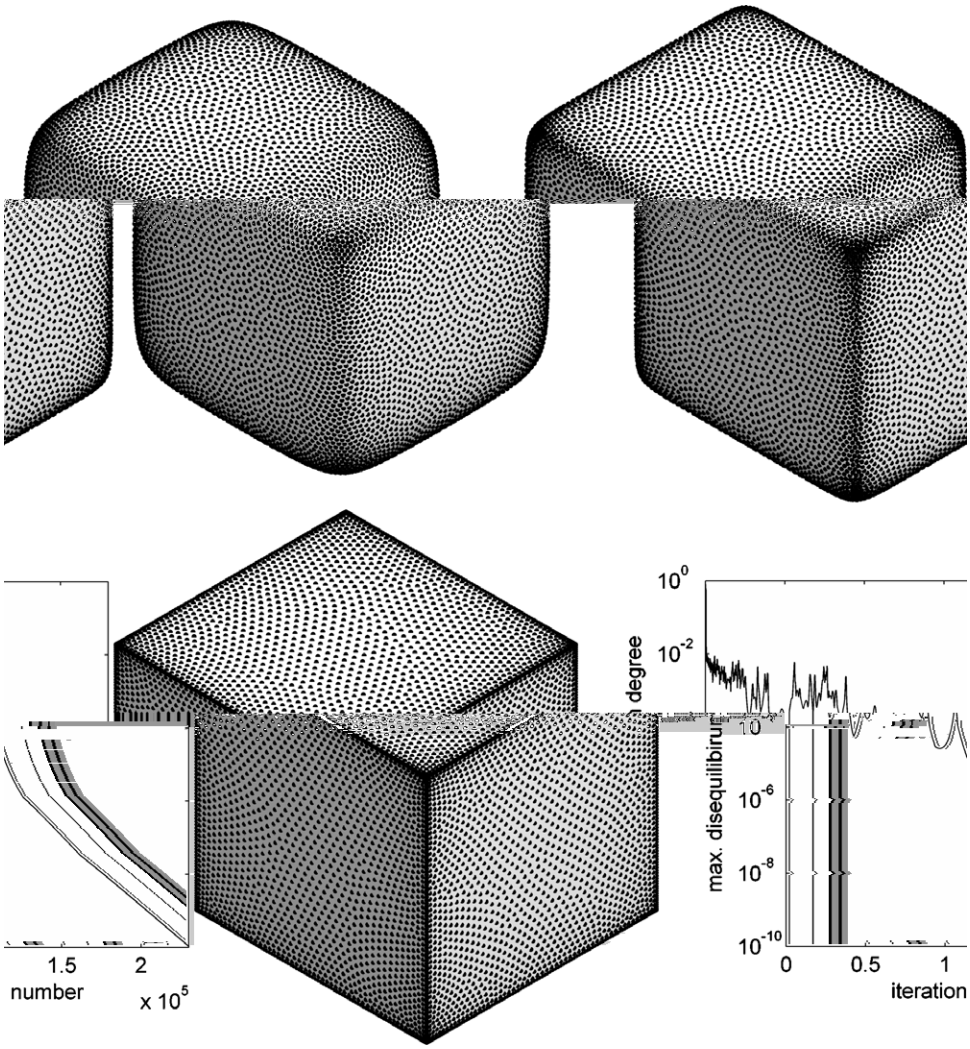

Fig. 11. Approximating configurations, final near local-minimum configuration and convergence of the algorithm for the problem of the Fekete points of the unit cube with $N = 10537$ and the Newtonian kernel.

calculation. In addition, the typical convergence behavior described in Section 3 can be observed. It is clear that almost the whole second half of the convergence path is in linear tendency.

Next we show the quality of the solutions provided by our algorithm by analyzing the interior field and the electrostatic charge density of the cube. Our estimations agree with some theoretical and numerical results due to other authors. For instance, Korevaar and Monterie, in [12, Theorem 1.2], obtained the following result involving the interior field. If x is a point in the interior of the solid cube, $d_x = d(x, \mathscr{S})$ and F_x^N is the field due to ω_N at x – *i.e*, the force that would act on a unitary charge on x due to N equal charges of magnitude $\frac{1}{N}$ located at ω_N – then there exists a scalar c such that for each $N \geqslant 2$,

$$|F_x^N| \leqslant c \frac{1 + d_x}{d_x^3} \frac{1}{\sqrt{N}}.$$

Fig. 12 (up) shows the maximum value of $\frac{d_x^3 |F_x^N|}{1+d_x}$ in the interior of the cube for different configurations of N points covering three orders of magnitude. Each maximum is obtained by evaluating in almost 10^5 points. It must be observed that a value of c for all N in the cube can be determined from the trivial case $N = 2$. How-

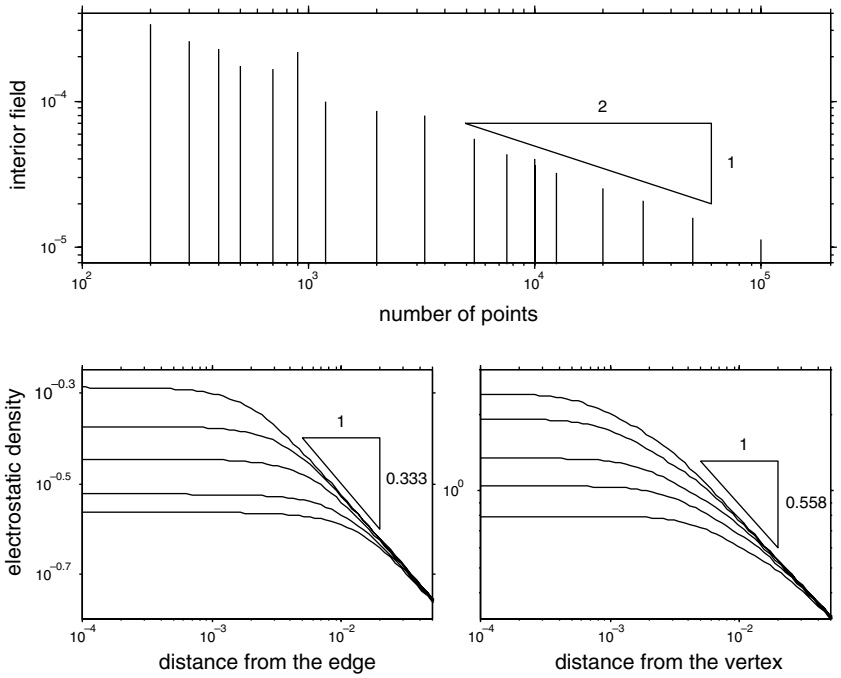

Fig. 12. Approximation of the interior field and the electrostatic charge density of the unit cube by means of our estimations of Fekete points.

ever, this value is excessively conservative for large N. For this reason, the first values of N have not been considered in the figure. In any case, our calculations sharply fit the order $\frac{1}{\sqrt{N}}$. In fact, for N sufficiently large, we propose $c = 0.036$.

A major open question is to obtain the electrostatic charge density of a cube. A theoretical analysis of the asymptotic behavior of the electrostatic charge density near the edges and the vertices of conductor bodies was done by Fichera in [6]. The obtained results were applied to the unit cube in [7]. The problem has been also treated by means of different numerical techniques. For instance, in [15], it was analyzed the dependence of the density on the distance r from points along the middle line of a face to an edge and on the distance from points along the diagonal of a face to a vertex. Moreover, it was showed numerical evidence of the fact that this dependence has the form $\alpha r^{-\frac{1}{3}}$ for the former and $\beta r^{-0.558}$ for the latter. In Fig. 12 (down) we give approximations of the electrostatic charge density near an edge and near a vertex of the unit cube for $N = 5000, 10000, 20000, 50000$ and 100000, and we compare they with the estimation given in [15]. The approximating curves have been obtained by evaluating the normal component F^n of the total force due to the N charges – of value $\frac{1}{N}$ – at points on $\mathscr{S}$ located along the middle line of a face and along a diagonal. The values of the density presented are $\frac{|F^n|}{2\pi}$. The density given by our configurations tends, although very slowly, to the estimations that appear in the literature. We want to note here that the objective of this study is to evaluate the suitability of the configurations obtained with our algorithm, and not to carry out an accurate asymptotic analysis of the electrostatic charge density of the cube.

6.2. Kelvin polyhedron

By analyzing the case of the Archimedean Kelvin Polyhedron we want to show that our configurations keep properties like the symmetries and proportions of the considered W-compact set. For this case, the approximating surfaces have been constructed by combining the planes corresponding to the different faces. We used the following implicit expression

$$f_p(x,y,z) = e^{p(x-0.5)} + e^{p(y-0.5)} + e^{p(z-0.5)} + e^{-p(x+0.5)} + e^{-p(y+0.5)} + e^{-p(z+0.5)} + e^{p(x+y+z-0.75)} + e^{p(-x+y+z-0.75)} + e^{p(x-y+z-0.75)} + e^{p(-x-y+z-0.75)} + e^{p(x+y-z-0.75)} + e^{p(-x+y-z-0.75)} + e^{p(x-y-z-0.75)} + e^{p(-x-y-z-0.75)} = 1$$

with $p = 25, 60$.

Fig. 13 shows a near local-minimum configuration of 10000 points on the Kelvin Polyhedron. In Table 4, we present the evolution of three ratios, r_1, r_2 and r_3, involving the number of points belonging to different faces of the polyhedron. If n_s^i, $i = 1, \ldots, 6$, denotes the number of points belonging to each square and n_h^j, $j = 1, \ldots, 8$, represents the number of points belonging to each hexagon, then $r_1 = \min \frac{n_s^i}{n_s^j}$, $r_2 = \min \frac{n_h^i}{n_h^j}$ and $r_3 = \min \frac{n_h^i}{n_s^j}$.

Table 4 also includes the evolution of the charge recovered by integrating the electrostatic density given by different configurations. In this case, a continuum estimation of the electrostatic density has been constructed from the Delaunay triangulation associated to the points in each face. The density value on each point x_i has been calculated as $\frac{|F_i|}{2\pi N}$, and these values have been linearly interpolated in each triangle. Let us note that, in spite of that this approach is very simple, the charge recovered for the distribution of 100000 points is more than the 99%.

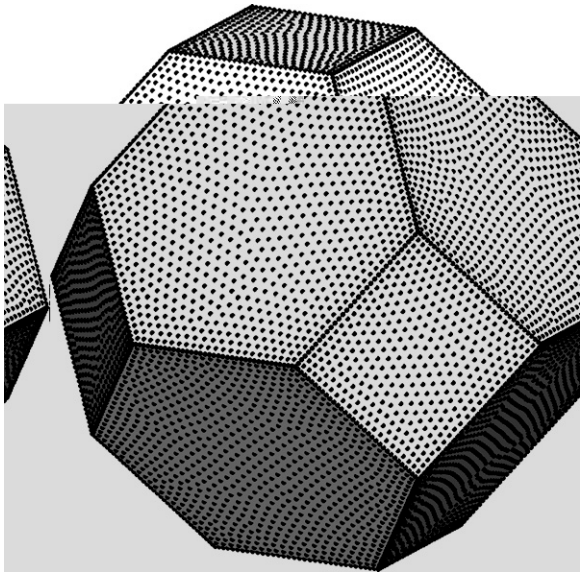

Fig. 13. A configuration in linear tendency on the Kelvin Polyhedron for $N = 10000$ with the Newtonian kernel.

Table 4
Geometrical ratios and charge recovered

N	r_1	r_2	r_3	q
5000	0.9884	0.9852	2.0618	0.9713
10000	0.9919	0.9923	2.0994	0.9788
20000	0.9947	0.9956	2.1300	0.9840
50000	0.9982	0.9986	2.1669	0.9893
100000	0.9984	0.9989	2.1816	0.9922

6.3. A more general example

Let us consider the sphere, the square and the curve defined respectively by

$$A = \left\{(x,y,z) \in \mathbb{R}^3 : (x-0.75)^2 + (y-0.75)^2 + (z+0.2)^2 = 0.64\right\},$$
$$B = \left\{(x,y,z) \in \mathbb{R}^3 : \max\{|x|,|y|\} \leqslant 1, z = 0\right\},$$
$$C = \left\{(x,y,z) \in \mathbb{R}^3 : \max\{|x-0.5|,|z|\} = 0.5, y = -0.5\right\}.$$

We analyze the Fekete point problem for the W-compact set $\mathscr{S} = A \cup B \cup C$. This example combines the three cases presented in Section 5.2; *i.e*, a surface that is the boundary of an open set, a surface with boundary and a curve.

It must be taken into account that the electrostatic charge density in the part of B inside the sphere A, that we denote by D, is necessarily null. For this reason, it is not necessary to consider D when the Newtonian kernel is used. In fact, we have carried out some numerical experimentation with this kernel including D in the set $\mathscr{S}$, and we have observed that, effectively, the particles leave D. On the other hand, D must be explicitly considered when other kernels are used, and then the approximating surfaces require to be connected in a similar way to the one indicated in Section 5.1.

For the construction of the approximating surfaces, we have used the following implicit functions,

$$f_1(x,y,z) = \mathrm{e}^{2p(x^2-1)} + \mathrm{e}^{2p(y^2-1)} - 1, \quad f_2(x,y,z) = \mathrm{e}^{2pz} - 1,$$
$$f_3(x,y,z) = (x-0.75)^2 + (y-0.75)^2 + (z+0.2)^2 - 0.64,$$
$$f_4(x,y,z) = \mathrm{e}^{pf_3(x,y,z)} - 1, \quad f_5(x,y,z) = \mathrm{e}^{2p(x+0.5)^2-0.25} + \mathrm{e}^{2pz^2-0.25} - 1,$$
$$f_6(x,y,z) = \mathrm{e}^{2p(y+0.5)} - 1, \quad f_7(x,y,z) = (x-h)^2 + (y-h)^2 + z^2,$$

where $h = 0.75 - \sqrt{0.3}$.

In these conditions, the implicit expression of the approximating surfaces used when D is not considered is

$$f_p(x,y,z) = \mathrm{e}^{-pf_2^2(x,y,z)+f_1(x,y,z)} + \mathrm{e}^{-pf_3(x,y,z)} + \mathrm{e}^{-p(f_6^2(x,y,z)+f_5^2(x,y,z))+1} = 1.$$

If D is included in the analysis, the corresponding expression is

$$f_p(x,y,z) = \frac{1}{\mathrm{e}^{-pf_2^2(x,y,z)+f_1(x,y,z)} + \mathrm{e}^{-pf_4^2(x,y,z)+1} + \mathrm{e}^{-p(f_6^2(x,y,z)+f_5^2(x,y,z))+1}} + \mathrm{e}^{-3pf_7(x,y,z)+1} = 1.$$

Fig. 14 shows a good configuration of 2000 points on $\mathscr{S}$. The effect of connecting conductor bodies with different dimensions can be observed. The repulsion of the sphere predominates over the repulsion of the square, and also the repulsion of the square predominates over the repulsion of the curve.

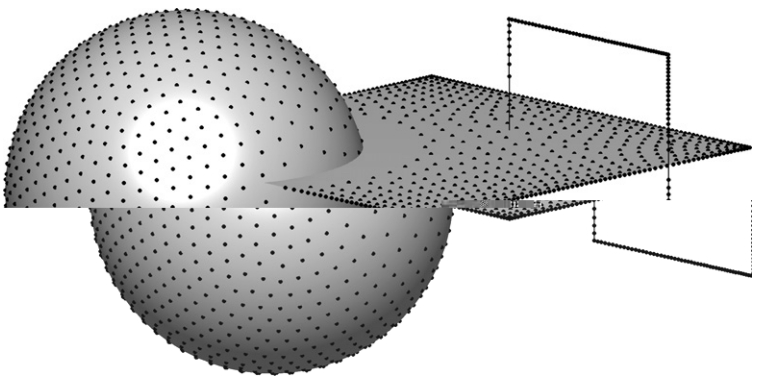

Fig. 14. Good configuration of $N = 2000$ points on $\mathscr{S}$ for the Newtonian kernel.

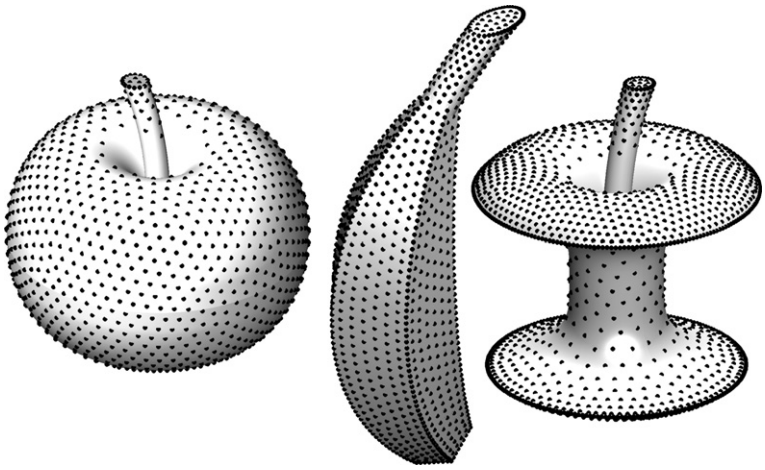

Fig. 15. A Newtonian still life.

It is important to note that in the approximation process corresponding to this case an object formed by pieces with different dimensions is being covered by a single surface. This fact requires to choose carefully the local degree of approximation to each one of the pieces. In this exercise we have used the approximating surfaces obtained by taking $p = 13.5, 15$ in the above expression.

6.4. A still life

We present here a funny exercise that shows the adaptability of the proposed technique to a great variety of geometries. We have composed a still life with near local-minimum configurations for the Newtonian kernel of 1500 points on a whole apple, 2500 points on a bitten apple and 1500 points on a Canary banana. Although the three objects have been treated individually, we present all of them in Fig. 15.

The approximating surfaces of the apples are based in the following implicit functions,

$$f_1(x,y,z) = \left(\frac{\sqrt{x^2+y^2}-1.5}{1.4}\right)^2 + \left(\frac{z-0.15}{2}\right)^2 - 1,$$

$$f_2(x,y,z) = \sqrt{x^2+y^2} - 1.6\left(\frac{z}{1.65}\right)^4 - 0.8,$$

$$f_3(x,y,z) = x^2 + \left(\sqrt{(y-7)^2+(z-1)^2} - 7\right)^2 - r^2,$$

$$f_4(x,y,z) = x^2 + y^2 + (z+1)^2 - 0.36,$$

where $r = 1.5 - 1.4\sqrt{0.819375}$.

The implicit equations of the approximating surfaces for the whole apple and for the bitten apple are, respectively,

$$f_p(x,y,z) = \mathrm{e}^{-pf_1(x,y,z)} + \mathrm{e}^{-pf_4(x,y,z)} + \frac{1}{\mathrm{e}^{1.5pf_3(x,y,z)} + \mathrm{e}^{-1.5pz} + \mathrm{e}^{1.5p(z-3.5)}} = 1$$

and

$$f_p(x,y,z) = \frac{1}{\mathrm{e}^{pf_1(x,y,z)} + \mathrm{e}^{pf_2(x,y,z)}} + \mathrm{e}^{-pf_4(x,y,z)} + \frac{1}{\mathrm{e}^{1.5pf_3(x,y,z)} + \mathrm{e}^{-1.5pz} + \mathrm{e}^{1.5p(z-3.5)}} = 1.$$

For the Canary banana, the corresponding implicit expression is

$$f_p(x,y,z) = \frac{1}{\sum_{i=1}^{5}\mathrm{e}^{pf_i(x,y,z)} + \mathrm{e}^{-p(\sin(0.175\pi)x+\cos(0.175\pi)z)}} + \frac{1}{\mathrm{e}^{pf_6(x,y,z)} + \mathrm{e}^{-pz} + \mathrm{e}^{p(z-4)}} = 1,$$

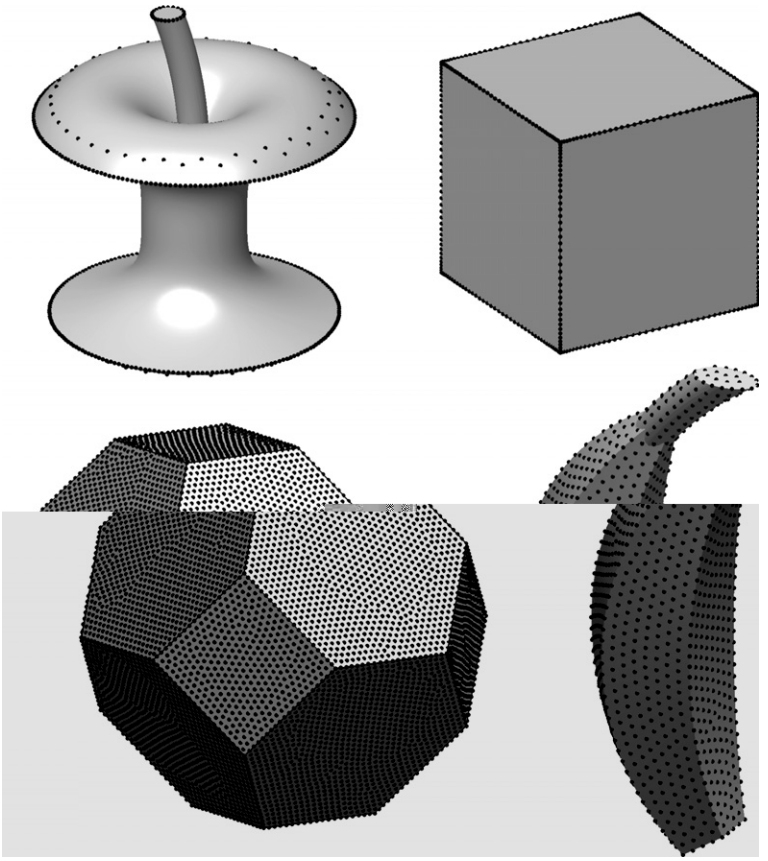

Fig. 16. Some examples of the application of the algorithm with $s = 0$ (up), $s = 2$ (down to the left) and $s = 3$ (down to the right).

where, for each $i = 1, \ldots, 5$,

$$f_i(x,y,z) = \cos\left(\frac{2\pi i}{5}\right)\left(5 - \sqrt{x^2+z^2}\right) - \sin\left(\frac{2\pi i}{5}\right)y + 0.75\left(\frac{16}{\pi^2}\arctan^2\left(\frac{z}{x}\right) - 1\right)$$

and $f_6(x,y,z) = y^2 + (\sqrt{x^2+z^2} - 5)^2 - 0.125$.

6.5. Other kernels

We conclude this paper by showing some configurations in linear tendency for kernels other than the Newtonian. We remark that the general behavior of our algorithm is essentially the same independently of the considered kernel. Fig. 16 shows a bitten apple and a cube with $N = 500$ and the logarithmic kernel, a Kelvin polyhedron with $N = 10000$ and the Riesz's kernel with $s = 2$ and a Canary banana with $N = 1500$ and the Riesz's kernel with $s = 3$.

These numerical results agree with the ones exposed in [10,11,25] about the reduction of the measure support corresponding to the logarithmic kernel and about the asymptotical uniform distribution of the points on a manifold with Hausdorff dimension d when $s \geqslant d$. It must be noted the high concentration of points on the singularities for the logarithmic kernel and the high degree of uniformity for $s \geqslant 2$ even on the singularities.

Acknowledgments

The authors express their sincere gratitude to Professor Antonio Gens for his unconditional support. This work has been partially supported by the CICYT under Project BFM2003-06014.

References

[1] M. Atiyah, P. Sutcliffe, The geometry of points particles, R. Soc. Lond. Proc. Ser. A Math. Phys. Eng. Sci 458 (2002) 1089–1115.
[2] M. Atiyah, P. Sutcliffe, Polyedra in physics, chemistry and geometry, Milan J. Math. 71 (2003) 33–58.
[3] E. Bendito, A.M. Encinas, Minimizing energy on locally compact spaces: existence and approximation, Numer. Funct. Anal. Optimiz. 17 (9–10) (1996) 843–865.
[4] J.F. Blinn, A generalization of algebraic surface drawing, ACM Trans. Graph. 1 (1982) 235–256.
[5] S.B. Damelin, P.J. Grabner, Energy functionals, numerical integration and asymptotic equidistribution on the sphere, J. Complexity 19 (2003) 231–246.
[6] G. Fichera, Comportamento asintotico del campo elettrico e della densita elettrica in prossimita dei punto singolari della superficie conduttore, Rend. Seminario Mat. dell'Universita e del Politecnico di Torino 32 (1973–1974) 111–143.
[7] G. Fichera, M.A. Sneider Ludovici, Distribution de la charge électrique dans le voisinage des sommets et des arêtes d'un cube, C.R. Acad. Sci. Paris 278 (A) (1974) 1303–1306.
[8] B. Fuglede, On the Theory of Potentials in locally compact spaces, Acta Math. 103 (1960) 139–215.
[9] D.P. Hardin, E.B. Saff, Discretizing manifolds via minimum energy points, Notices Amer. Math. Soc. 51 (2004) 1186–1194.
[10] D.P. Hardin, E.B. Saff, Minimal Riesz energy point configurations for rectificable *d*-dimensional manifolds, Adv. Math. 193 (2005) 174–204.
[11] D.P. Hardin, E.B. Saff, H. Stahl, The support of the logarithmic equilibrium measure on sets of revolution in $\mathbb{R}^3$, preprint.
[12] J. Korevaar, M.A. Monterie, Approximation of the equilibrium distribution by distributions of equal point charges with minimal energy, Trans. Amer. Math. Soc. 350 (1998) 2329–2348.
[13] A.B.J. Kuijlaars, E.B. Saff, Asymptotics for minimal discrete energy on the sphere, Trans. Amer. Math. Soc. 350 (1998) 523–538.
[14] N.S. Landkof, Foundations of Modern Potential Theory, Springer-Verlag, 1972.
[15] M. Mascagni, N.A. Simonov, The random walk on the boundary method for calculating capacitance, J. Comput. Phys. 195 (2004) 465–473.
[16] K.J. Nurmela, Constructing spherical codes by global optimization methods, Helsinki University of Technology, Series A: Research Reports, 32 (1995).
[17] P.O. Persson, G. Strang, A simple mesh generator in MATLAB, SIAM Rev. 46 (2) (2004) 329–345.
[18] E.A. Rakhmanov, E.B. Saff, Y. Zhou, Minimal discrete energy on the sphere, Math. Res. Lett. 1 (1994) 647–662.
[19] E.B. Saff, A.B.J. Kuijlaars, Distributing many points on a sphere, Math. Intell. 19 (1997) 5–11.
[20] E.B. Saff, V. Totik, Logarithmic Potentials with External Fields, Springer-Verlag, 1997.
[21] K. Shimada, D.C. Gossard, Automatic triangular mesh generation of trimmed parametric surfaces for finite element analysis, Comp. Aid. Geomet. Des. 15 (1998) 199–222.
[22] S. Smale, Mathematical problems for the next century, Math. Intell. 20 (1998) 7–15.
[23] A.Witkin, P. Heckbert, Using particles to sample and control implicit surfaces, in: Computer Graphics Proceedings SIGGRAPH 94, 1994, pp. 269–278.
[24] R. Womersley, <http://web.maths.unsw.edu.au/rsw/Sphere/Energy/index.html>.
[25] R. Womersley, <http://web.maths.unsw.edu.au/rsw/Torus/>.
[26] Y. Zhou, Arrangements of Points on the Sphere, Ph.D. Department of Mathematics, University of South Florida, 1995.